



INTERNATIONAL ATOMIC ENERGY AGENCY  
UNITED NATIONS EDUCATIONAL, SCIENTIFIC AND CULTURAL ORGANIZATION  
**INTERNATIONAL CENTRE FOR THEORETICAL PHYSICS**  
I.C.T.P., P.O. BOX 586, 34100 TRIESTE, ITALY, CABLE: CENTRATOM TRIESTE



H4.SMR/845-12

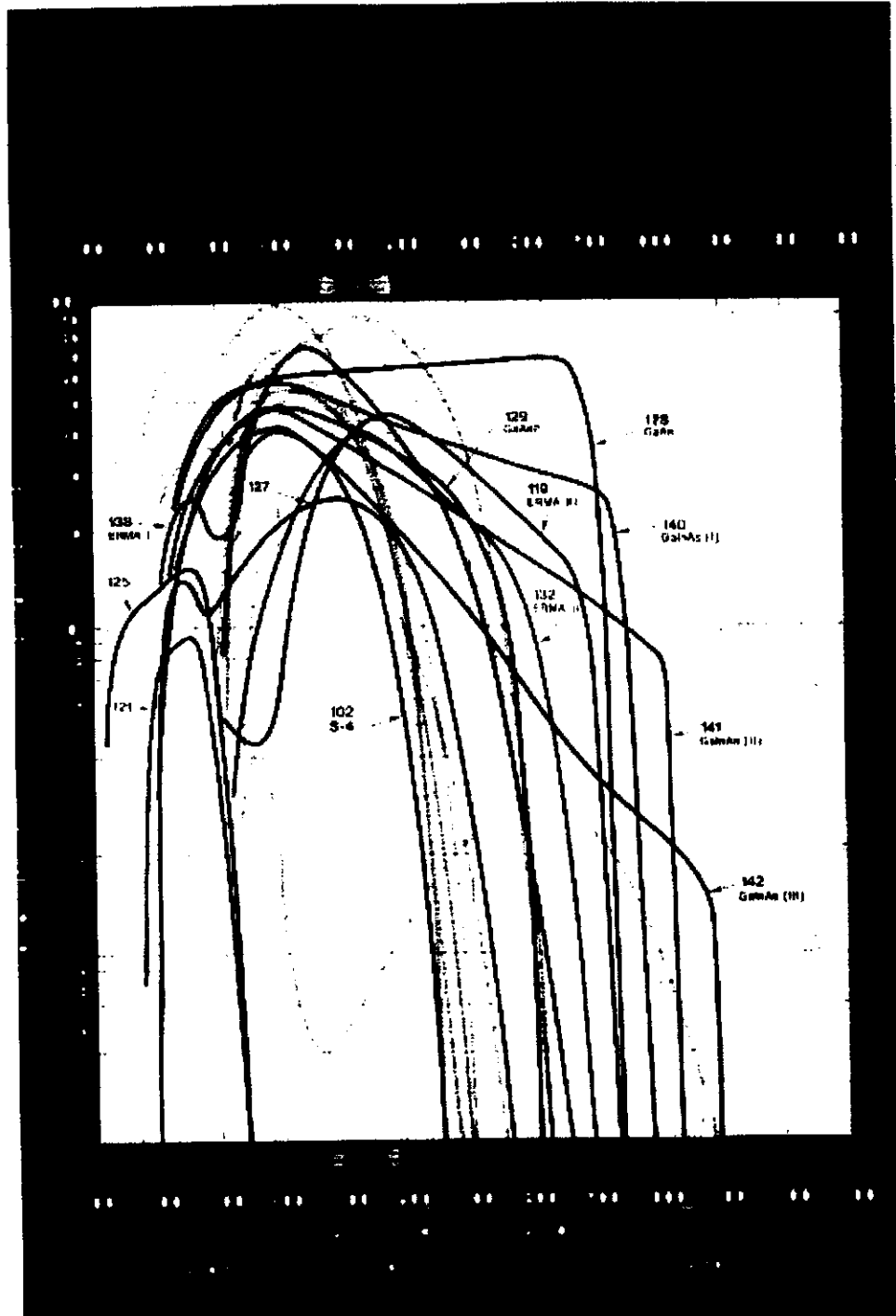
**Second Winter College on Optics**

20 February - 10 March 1995

***Detectors***

**G. Longobardi**

**Istituto Nazionale di Ottica  
Arcetri, Firenze, Italia**



## DETECTORS

*Seminar Lessons: Giuseppe Longobardi*

*Laboratory Tutor: Claudio Ciamberlini*

Istituto Nazionale di Ottica  
Largo Enrico Fermi, 6 - Arcetri  
50125 - Firenze - IT  
Tel.: +39 55 23081  
Fax: +39 55 2337755  
E-mail: opus@fox.ino.it

### Biography:

**Giuseppe Longobardi** received a degree in Electronic Engineering from the Polytechnic of Torino (Italy). At present he is working as Research Director at the National Institute of Optics in Florence. He is also Director of Consortium CEO, which is a Joint: University - Research Centres - Industry in Florence. CEO produces and develops the scientific research and technological innovations in the optoelectronic field. He has been teaching at the Graduate School of Optics at Florence University since 1980. His main research interests are optical sensors, imaging system, semiconductor lasers and robotics. He is also author of numerous articles in international scientific journals.

**Claudio Ciamberlini** obtained the degree in Physics in 1991 at Florence University. He obtained the graduate degree in 1994 at the Graduate School in Optics at Florence University. He is working on low light level imaging for ophthalmic applications, and on optoelectronic system control in textile field in BRITE-EURAM project of the European Community.

## Index:

1. Photon detectors, 1
2. Photoemissive detectors, 1
- 2.1 Vacuum phototubes, 1
3. Photocathode, 3
- 3.1. Photocathode materials, 6
- 3.2. The spectral response, 9
- 3.3. Dark current, 10
4. Vacuum photodiodes, 11
- 4.1. Signal to noise ratio, 13
5. Photomultiplier Tubes, 14
- 5.1. Cathode- first dynode stage, 16
- 5.2. Dynode chain, 17
- 5.3. Last dynode-anode stage, 17
- 5.4. Anode dark current, 18
6. Single Electron Response (SER), 18
7. Noise in the photomultiplier, 20
8. Signal-to-noise ratio of photomultiplier tubes, 21
9. Time characteristics, 22
10. Photomultiplier operation, 23
11. Image-Intensifier technique, 28
12. Gain, 28
13. Zero generation of image intensifier tube, 29
14. First generation of image intensifier tube, 29
15. Second generation of image intensifier tube, 30
- 15.1 Electrons lens of image intensifier inverter tube, 32
- 15.2 Channel plate of image intensifier inverter tube, 33
- 15.3 Phosphor screen of image intensifier inverter tube, 35
- 15.4 Modulation transfer function of image intensifier inverter, 35
16. Third generation of image intensifier tube, 36

Laboratory Guide, 37

Introduction, 37

Instruments background, 37

- 1) Acquisition driver, 37
- 2) Monochromator, 38
- 3) Semiconductors photodiode, 41
- 4) Photomultiplier, 42
- 5) Image intensifier tube, 43

Experiments description, 43

Spectral Sensitivity of photomultiplier, 43

Noise Equivalent Power (NEP), 44

Single Electron Response (SER) observing, 45

Use of an second generation image intensifier, 45

Appendix: A. Single current on the different dynodes of photomul, 46

## 1. Photon detectors

Photon detectors are used in radiometry to produce an electrical signal in response to radiant energy.

The primary detection mechanism is the photoelectric effect by which a photon of light is absorbed and excites an electron to a higher energy state.

Photon detectors generate an electric signal by means of two main processes:

1) external photoelectric effect in which a photoelectron is emitted by a photoemitting material generally into the vacuum and captured by a second electrode as in phototubes and photomultipliers.

2) internal photoelectric effect in which an electron is excited to move from one energy level to another, higher level. During this process the electric charge carriers (electrons and holes) remain inside the material and either change its conductivity or generate a voltage. These detectors consist either of a uniform material (bulk detectors) such as photoconductors or of a junction between two dissimilar materials such as junction photodiodes (pin, avalanche ....).

In general the spectral responsiveness of photon detectors is selective because it is determined mainly by the chemical-physical composition of the materials used to absorb photons.

The purpose of my lectures is to present these physical processes and operating considerations on photodetectors of the first kind for the wavelength range between 100 nm and 1  $\mu$ m.

## 2. Photoemissive detectors

### 2.1 Vacuum phototubes

All materials have a photoemissive effect: if they are exposed to electromagnetic radiation of sufficient energy, they eject electrons. Simply speaking, the electronic emission mechanism includes the sequence of three steps:

a) Photon absorption.

b) Energy transfer to an electron. The electron absorbing this energy obtains kinetic energy and moves to the surface of the material.

c) Electrons pass over the surface of a retaining potential called "work function" and escape from the material.

Each step involves losses which affect the system's efficiency.

a) In the first phase not all photons are absorbed some are reflected at the surface, others for very thin materials cross the body without interaction with it.

b) In the second phase the excited photoelectrons, lose their energy because of the scattering electron-electron or electron-phonon or electron impurities.

c) In the third phase the residual energy of the photoelectron must be used to pass over the retaining potential of the surface  $E_w$ .

So, not all photons produce photoelectrons and not all photoelectrons produced are emitted. The mean ratio between the number of photoelectrons emitted and the number of photons incident is called quantum efficiency  $\eta$ ; it depends in a complex way on the type of material, on its thickness, on the chemical-physical characteristics of its surface, on the photon energy and also on geometric aspects such as angle of incidence of the radiation.

Photoemissive effects occur in certain conductors or metals and in semiconductors. In these materials, incident photons which are not reflected at the surface, penetrate to some depth the material where they are absorbed.

Each photon carries an energy that is described by Planck's equation:

$$E = h\nu = \frac{hc}{\lambda} \quad (1)$$

where :  $h = 6.623 \cdot 10^{-34}$  Wsec<sup>2</sup> (Planck's constant)

$\nu$  = radiation frequency

$c = 2.998 \cdot 10^{10}$  cmsec<sup>-1</sup> (electromagnetic radiation speed)

$\lambda$  = radiation wavelength

All photosensitive materials used for detectors are semiconductors. The semiconductor work functions allow operation at longer wavelengths than is possible with metals. Metal material does not always respond to photon wavelengths longer than 0.3  $\mu\text{m}$  and these photocathodes are used as ultraviolet detectors.

In semiconductors  $E_w$  consists of two components (Fig.1): the electron affinity  $E_a$  (which is the energy difference between the vacuum potential and the conduction band  $E_a = E_{vac} - E_c$ ) and part of the band-gap energy  $E_g$  (which is that  $E_w = E_a + E_g$ ).

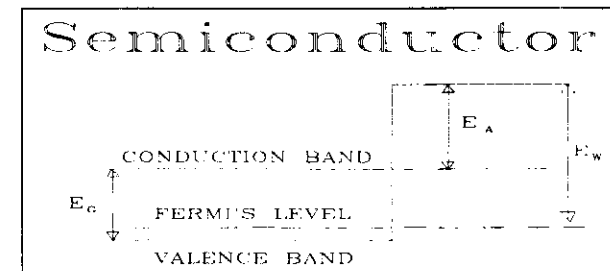


Fig.1

Thus, the probability of an electron escaping from the materials is not zero if its radiant energy  $h\nu$  exceeds the electronic affinity  $E_a$ , when it enters the conduction band; i.e. if the photon's radiant energy  $E_{ph}$  is:

$$E_{ph} \geq E_a + E_g \quad (2)$$

then the effect of photoelectric emission sets in.

The equation (2) indicates that the quantum efficiency of the system is equal to zero for radiant energies less than  $E_a + E_g$ .

In other words the detector has a threshold which is usually expressed through the maximum wavelength at which it is sensitive:

$$\lambda_{max} = \frac{1.98 \cdot 10^{-15} (J \cdot nm)}{E_a + E_g} \quad (3)$$

A separate type of semiconducting photocathode that exhibits relatively long-wavelength response at high quantum efficiency is said to have negative electron affinity (NEA)

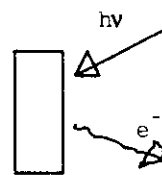
Therefore, negative electron affinity implies that the threshold energy is now:

$$E_{ph} \geq E_a \quad (4)$$

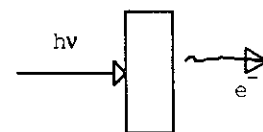
### 3. Photocathode

The photocathode is an electrode which emits photoelectrons, if hit by photons. There are two different photocathode configurations:

1) opaque photocathode, deposited on a thick metallic substrate where the electrons are emitted from the irradiated surface



2) semitransparent photocathode, vacuum deposited at the glass window of the envelope, where the electrons are emitted from the opposite surface that irradiated



The thickness of the semitransparent photocathode is critical. Greater or smaller thicknesses reduce efficiency for opposite reasons: in the former thickness can exceed the escape depth of electrons, in the latter a fraction of the radiation is transmitted and does not contribute to the photoemissive process. In both configurations the electromagnetic radiation reach as the photoemissive material through a "window" of transparent material. The window material produces the detector response at the short wavelength. The spectral transmittance characteristics of various window materials are shown in Fig. 2.

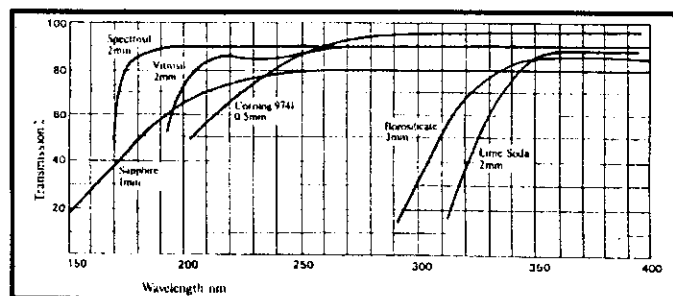


Fig. 2

The Electronics Industries Association (EIA) registered several relative spectral responsivity functions of photoemissive detectors by their so called "S" number which specifies the spectral responsivity distribution of both the photocathode and the window material. Some details of a commonly used S number are listed in table 1.

Table 1:

Characteristics of Various Photocathodes <sup>a</sup>									
Material Composition	Response Designation	Type of Photocathode	Envelope Material <sup>b</sup>	Conversion Factor <sup>c</sup> (A/mm <sup>2</sup> /watt at $\lambda_{max}$ )	Sensitivity (A/mm <sup>2</sup> )	Wavelength of Maximum Response, $\lambda_{max}$ (nm)		Quantum Efficiency at $\lambda_{max}$ (percent)	Dark Current at $\lambda = 25^\circ C$ $\Delta \times 10^{-11}/cm^2$
						Minimum Response, $\lambda_{min}$ (nm)	Maximum Response, $\lambda_{max}$ (nm)		
Ag-O-Cs	S-1	O	0080	92.7	25	800	2.3	0.36	900
Ag-O-Rb	S-3	O	0080	285	6.5	420	1.8	0.55	—
Cs <sub>3</sub> Sb	S-19	O	SiO <sub>2</sub>	1603	40	330	64	24	0.3
Cs <sub>3</sub> Sb	S-4	O	0080	1044	40	400	42	13	0.2
Cs <sub>3</sub> Sb	S-5	O	9741	1262	40	340	50	18	0.3
Cs <sub>3</sub> Bi	S-8	O	0080	757	3	365	2.3	0.77	0.13
Ag-Bi-O-Cs	S-10	S	0080	509	40	450	20	5.6	70
Cs <sub>3</sub> Sb	S-13	S	SiO <sub>2</sub>	799	60	440	48	14	4
Cs <sub>3</sub> Sb	S-9	S	0080	683	30	480	20	5.3	—
Cs <sub>3</sub> Sb	S-11	S	0080	808	60	440	48	14	3
Cs <sub>3</sub> Sb	S-21	S	9741	783	30	440	23	6.7	—
Cs <sub>3</sub> Sb	S-17	O'	0080	667	125	490	83	21	1.2
Na <sub>2</sub> KSb	S-24	S	7056	1505	32	380	64	23	0.0003
K-Cs-Sb	—	S	7740	1117	30	400	89	28	0.02
(Ca)Na <sub>2</sub> KSb	—	S	SiO <sub>2</sub>	429	150	420	64	18.9	0.4
(Cs)Na <sub>2</sub> KSb	S-20	S	0080	428	150	420	64	19	0.3
(Cs)Na <sub>2</sub> KSb	S-25	S	0080	276	160	420	44	13	—
(Cs)Na <sub>2</sub> KSb	ERMA <sup>d</sup>	S	7056	169	265	575	45	10	1
Ga-As	—	O'	9741	148	250	450	37	10	0.1
Ga-As-P	—	O'	Sapphire	310	200	450	61	17	0.01
InGaAs-CsO'	—	O'	0080	266	260	400	71	22	14
Cs <sub>2</sub> Te	—	S	LiF	/	/	120	12.6	13	9
CsI	—	S	LiF	/	/	120	24	20	9
CuI	—	S	LiF	/	/	150	13	10.7	9

### 3.1. Photocathode materials (from Hamamatsu)

Most photocathodes are made of a compound semiconductor mostly consisting of alkali metals with a low work function. There are ten kinds of photocathodes which are currently in practical use. Each photocathode is available with a transmission (semitransparent) type or a reflection (opaque) type, with different device characteristics. At present, because many photocathode and window materials are available, the *S number* is not frequently used except for S-1, S-20, etc. The photocathode spectral response is instead expressed in terms of photocathode materials. The photocathode materials commonly used in photomultiplier tubes are as follows:

#### 1) Cs-I: Cs-I is insensitive to solar radiation and therefore called "solar blind".

Its sensitivity falls sharply at wavelength longer than 200 nm and it is exclusively used for vacuum ultraviolet detection. As window materials,  $MgF_2$  crystals or synthetic silica are used because of high ultraviolet transmittance. Although Cs-I itself has high sensitivity to wavelength shorter than 115 nm. This means that the spectral response of a photomultiplier tube using the combination of Cs-I and  $MgF_2$  covers a range from 115 to 200 nm. To measure light with wavelength shorter than 115 nm using Cs-I, an electron multiplier having a first dynode on which Cs-I deposited is often used with the input window removed.

#### 2) Cs-Te

Cs-Te is insensitive to wavelength longer than 300 nm and is also called "solar blind" just as with Cs-I. A special Cs-Te photocathode processed to have strongly suppressed sensitivity in the visible part of the spectrum has been manufactured. With Cs-Te, the transmission type shows the same spectral response range, but the reflection type exhibits twice the sensitivity of the transmission type. Synthetic silica or  $MgF_2$  is usually used for the input window.

#### 3) Sb-Cs

This photocathode has sensitivity in the ultraviolet to visible range, and is widely used in many applications. Because the resistance of the Sb-Cs photocathode is lower than that of the bialkali photocathode described later on, it is suited to applications where light intensity to be measured is relatively high, so that a large current can flow in the cathode, and is also used where changes in the photocathode resistance due to cooling affects measurements. Sb-Cs is chiefly used for the reflection type photocathode.

#### 4) Bialkali (Sb-Rb-Cs, Sb-K-Cs)

Since two kinds of alkali metals are employed, these photocathodes are called "bialkali". The transmission type of these photocathodes has a spectral response range similar to the Sb-Cs photocathode, but has higher sensitivity and lower dark current. It also provides sensitivity that matches the emission of  $NaI(Tl)$  scintillator, thus being widely used for scintillation counting in radiation measurements. On the other hand, the reflection-type bialkali photocathodes are intended for different applications and therefore are manufactured by a different process using the same materials. As a result, they offer enhanced sensitivity on the long wavelength side, providing a spectral response from the ultraviolet region to around 700 nm.

#### 5) High temperature, low noise bialkali (Sb-Na-K)

As with the above bialkali photocathodes, two kinds of alkali metals are used. The spectral response range of this photocathode is almost identical with that of the above bialkali photocathodes, but the sensitivity is somewhat lower. This photocathode can withstand operating temperatures of up to 175°C while normal photocathodes are guaranteed to no higher than 50°C. For this reason, it is ideally suited for use in oil well logging where photomultiplier tubes are often subjected to high temperatures. In addition, when used at room temperatures, this photocathode exhibits very low dark current, thus making it very useful in low-level light detection, for instance in photon counting applications where low noise is a prerequisite.

## 6) Multialkali (Sb-Na-K-Cs)

Since three kinds of alkali metals are employed, this photocathode is sometimes called a "trialkali". It has high sensitivity, wide spectral response from the ultraviolet through near infrared region around 850 nm, and is widely used in broad-band spectrophotometers. Furthermore, Hamamatsu also provides a multialkali photocathode with long wavelength response extending up to 900 nm, which is especially useful in the detection of chemiluminescence in  $\text{NO}_x$ , etc.

## 7) Ag-O-Cs

The transmission type photocathode using this material is sensitive from the visible through near infrared region, from 300 to 1200 nm, while the reflection type shows a slightly narrower region, spectral range from 300 to 1100 nm. Compared to other photocathodes, this photocathode shows lower sensitivity in the visible region, but has sensitivity at longer wavelengths in the near infrared region. Thus, both the transmission type and reflection type Ag-O-Cs photocathodes are chiefly used for near infrared detection.

## 8) GaAs (Cs)

A GaAs crystal activated with cesium is also used as a photocathode. The spectral response of this photocathode covers a wide range from ultraviolet through 930 nm with a plateau curve from 300 to 850 nm, showing a sudden cut-off at near infrared limit. It should be noted that if exposed to incident light with high intensity, this photocathode tends to suffer sensitivity degradation when compared with other photocathodes.

## 9) InGaAs (Cs)

This photocathode provides a spectral response extending further into the infrared region than the GaAs photocathode. Additionally, it offers a superior signal-to-noise ratio in the neighbourhood of 900 to 1000 nm in comparison with the Ag-O-Cs photocathode.

## 3.2. The spectral response

The main characteristics of spectral response are:

1. The quantum efficiency  $\eta$  (%) already defined in par.2
2. The radiant sensitivity  $R$  (A/W)

$R$  is the photoelectric current from the photocathode divided by the incident radiant flux at a given wavelength, expressed in units of Ampere per Watt. The expression for  $R$  as a function of quantum efficiency  $\eta$  is:

$$R = \frac{e\lambda}{hc} \eta$$
$$R = \frac{i_\lambda}{\Phi_\lambda} \quad i_\lambda = \frac{\eta e}{h\nu} \Phi_\lambda \quad (5)$$

The spectral response characteristics are shown in fig (3) where the lines at  $\eta=\text{constant}$  are represented

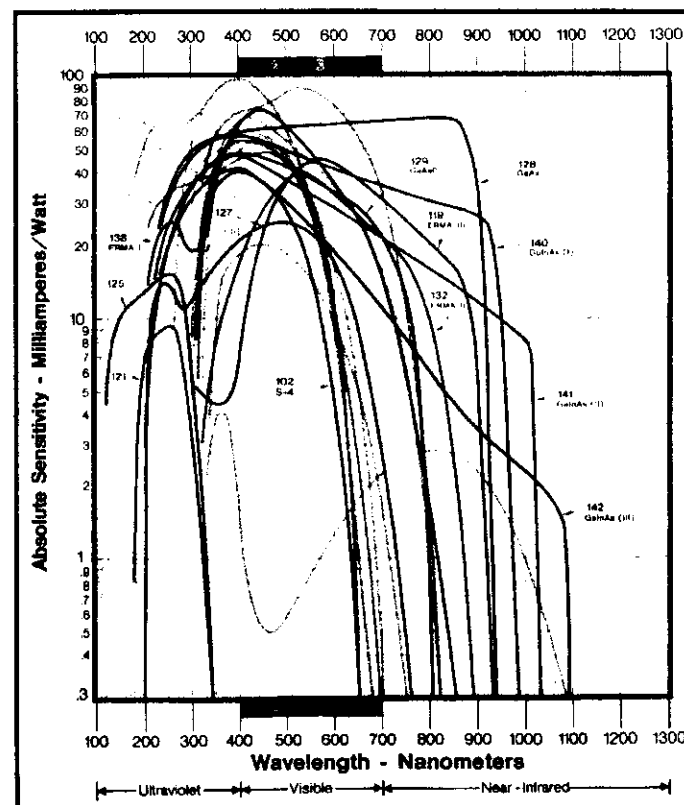


Fig. 3

The various types of photocathodes also differ from each other for a lot of important features such as dark current, stability, maximum current density, sensitivity to fatigue effects, etc.

### 3.3. Dark current

This is the amount of current which flows even when the photocathode operates in a complete dark state. The effect depends mainly on thermal emission current from the photocathode. Thermoelectronic emission is caused by the thermoelectrons excited from the valence band to the conduction band with enough energy for ejection.

Dark emission obviously depends on the temperature as follows:

$$J = 7.5 \cdot 10^{20} T^2 \exp(-\Psi/KT) \quad (6)$$

Where:  $J$  is the number of electrons per  $\text{cm}^2$

$T$  is the absolute temperature

$K$  is the Boltzmann const:  $1.38 \cdot 10^{-23}$  joule/k

$e$  is the electron charge ( $1.6 \cdot 10^{-19}$  coulomb)

$\Psi$  is work function

Eq. 6 also implies that the dark current decreases with decreasing temperature. Often dark emission is characterized by the mean value of the electronic current associated with it, i.e. the dark current. The noise during measurements is not caused by this mean current but by its fluctuations. The *rms* value (electrons involving the process) is given by:

$$i_d^2 = 2eI_d f \quad (7)$$

Where:  $I_d$  = means dark current,  $f$  = Bandwidth of the measuring circuit.

The maximum current density from a photocathode without damage for its surface, depends on both the emitting material and the substrate. All emitting materials, being semiconductors, have a resistivity from  $10^{-4}$  to  $10^7$ . This implies that the current greater than a fixed limit produce potential drops in the photocathode and then radial electrical fields which decrease the photoelectron

collection efficiency by the anode (in the case of phototube) or by the first dynode (in the case of photomultiplier). This is given by the temperature because the resistivity in a semiconductor decreases with it: the above mentioned current limit decreases for a lower temperature. We must take it into account when the photocathode is cooled in order to reduce thermoelectronic emission. The semitransparent photocathode limit current is usually lower than that of an opaque.

Fatigue is the changing of the output with time for a constant input. This is a change of the responsivity, mostly caused by the time of operation with high inputs. Fatigue is reversible, that is the sensitivity will return to the original sometime after the input optical signal that caused the fatigue is removed. Examples of variation are shown in fig. (4).

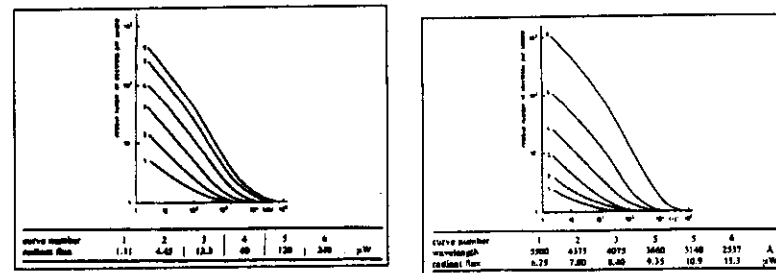


Fig. 4

### 4. Vacuum photodiodes

In vacuum photodiodes the photocathode is placed inside a vacuum tube with the anode placed at a few millimeters and biased positively with respect to it, as shown in fig. (5). The anode is the electrode which collects the electrons from the illuminated photocathode through an anode resistor  $R_L$  and produce the signal output, being biased positively with respect to the photocathode. The voltage drop  $V_O = i_p R_L$  across the load resistor is a measurement of the radiation hitting the photocathode.

Two basic groups of phototubes have been developed: low voltage (50-250V) groups and high voltage (1-5kV) biplanar phototubes designed for subnanosecond rise times and peak anode currents for short pulses of several amperes and pulsed laser detection. Technical data of high voltage phototubes are given in tables 2 and 3.

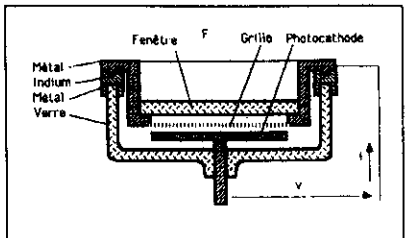


Fig. 5

Table 2:

Model	Cathode diameter [mm]	Spectral type	Operational voltage [V]	Rise time [ns]	Dark current [A]	Maximum voltage [V]
Amperex-Philips						
AVHC 201	102	S-4	2500	1.0	$1 \times 10^{-9}$	5000
XA 1003	20	S-1	1500	0.2	$5 \times 10^{-9}$	2500
Hamamatsu						
R 1193-03	32	S-20	—	0.3	$5 \times 10^{-9}$	2500
R 1328-03	10	S-20	—	0.09	$1 \times 10^{-9}$	2000
ITT Industrial Laboratories						
FW 114	44	S-4	2500	0.5	$5 \times 10^{-9}$	5000
FW 128	21	S-4	1000	0.7	$5 \times 10^{-9}$	2000
F 4007	152	S-4	2500	0.5	$5 \times 10^{-9}$	2000
F 4014	10	S-1	1000	0.1	$5 \times 10^{-9}$	2000

Table 3:

Model	Responsivity [ $\mu\text{A}/\text{W}$ ]	Maximum average current [ $\mu\text{A}$ ]	Maximum peak current [A]	Maximum cathode current density	Spectral response [ $\text{mA}/\text{W}$ ]
Amperex-Philips					
AVHC 201	35	10	10		30 at 437 nm
XA 1003	20	1	1		1.4 at 903 nm
Hamamatsu					
R 1193-03	60	50	1	0.12 $\text{W}/\text{mm}^2$	
R 1328-03	60	5	0.3	0.12 $\text{W}/\text{mm}^2$	
ITT Industrial Laboratories					
FW 114	30	75	5	5 $\mu\text{A}/\text{cm}^2$	
FW 128	30	18	0.5	5 $\mu\text{A}/\text{cm}^2$	
F 4007	30	900	60	5 $\mu\text{A}/\text{cm}^2$	
F 4014	10	0.35	0.1	5 $\mu\text{A}/\text{cm}^2$	

#### 4.1. Signal to noise ratio

Considering the radiant power  $\Phi$  as a stream of photons sinusoidally modulated at 100% with a mean value  $\Phi_s$ . The average current is given by:

$$I_s = e\eta\Phi_s \quad (8)$$

The  $I_{s(\text{eff})}$  is given by:

$$I_{s(\text{eff})} = \frac{1}{\sqrt{2}} e\eta\Phi_s \quad (9)$$

The noise associated with this current, for shot effect, is given by:

$$\bar{I}_s^2 = 2eI_s\Delta f \quad (10)$$

A noise current produced by Johnson noise relative to  $R_L$ :

$$\bar{I}_n^2 = \frac{4KT}{R_L} \Delta f \quad (11)$$

The processes are uncorrelated and statistically independent so:

$$\bar{I}_s^2 = 2eI_s\Delta f + \frac{4KT}{R_L} \Delta f \quad (12)$$

the signal to noise ratio is:

$$\frac{S}{N} = \frac{I_{s(\text{eff})}}{\sqrt{\bar{I}_s^2}} = \frac{e\eta\Phi_s / \sqrt{2}}{\left(2eI_s + \frac{4KT}{R_L}\right)^{\frac{1}{2}} \cdot \Delta f^{\frac{1}{2}}} \quad (13)$$

The weakest input that can be detected is the power input generating a signal of the same amplitude as the rms noise signal. the weakest signal detectable is that for which the signal to noise ratio is 1. the minimum power is called noise equivalent power (NEP). The NEP (in watts) is often specified normalized for unit bandwidth:

$$\Delta f = 1\text{Hz}; \quad \text{NEP} = I_s / R \quad (14)$$

with  $R$ =responsivity in  $\text{A}/\text{W}$ .

In our case:

$$\text{NEP} = \frac{(2eI_s + 4KT / R_L)^{\frac{1}{2}}}{\lambda e\eta / hc} \quad (15)$$

Let us calculate the factor under square root in case in which  $I_s$  is particularly high such as for the S<sub>1</sub> photocathode where  $I_s = 10^{-11} \text{ A}$ . For  $T=300^\circ\text{K}$  the under root expression becomes:

$$3.2 \cdot 10^{-30} + 1.6 \cdot 10^{-30} / R_L \quad (16)$$

Now we can ask ourselves for what value the thermal noise associated with  $R_L$  can be neglect with respect to the first term relative to the dark current,  $R_L$  must be greater than  $10^{11} \Omega$ .

In other words, in order for the behaviour of the system concerning the sensitivity limit to be determined only by the detector and not by the electronic external network, the load resistance value must be very high.

Apart from the difficulty of realizing and utilizing such resistance this would limit the bandpass of the device to very low frequencies, for example with a parasite capacitance of 5 pF, the time constant of RC lowpass filter would be  $\tau=5 \cdot 10^{-1}$  sec and the cut-off frequency  $f=0.3$  Hz.

It is clear that only for very low frequencies, that is for measurement in continuos, it is possible to utilize the inherent capability of the phototube for detecting very low signal otherwise the ultimate limit sensitivity is settled by external electronic network.

Since a phototube can be a very fast device (rise time up to ten psec.). The multiplication is that the phototube cannot be utilized with all its inherent capabilities: it can be utilized either as a detector with low noise for continuos measurements or to detect very fast signals of high intensity, where dark current and noise are of less importance. This drawback is overcome with the photomultiplier tube.

## 5. Photomultiplier Tubes

Photomultiplier tubes are detectors with a photoemissive cathode, a dynode system where the secondary effect provides amplification of the cathode current, and an anode that collects electrons from the dynode system yielding an output current (fig. 6). The photocathode is one of those already mentioned. The dynode is an electrode covered with special material with secondary emission.

An incident electron transfers its energy to electrons in the material, raising their energy to the extent that they can escape from the material. In semiconductors many more electrons reach the surface of the material with sufficient energy to

escape. The electric field must be applied to lead the electrons through the multiplier. the potential distribution and electrode structure of a photomultiplier tube is designed to be provide optimum performance. Major secondary emissive materials used for dynodes are alkali antimonide beryllium oxide (BeO), magnesium oxide (MgO), gallium phosphide (GaP) and gallium arsenide phosphide (GaAsP). The substrate electrode coated with these materials is made of nickel or copper beryllium alloy.

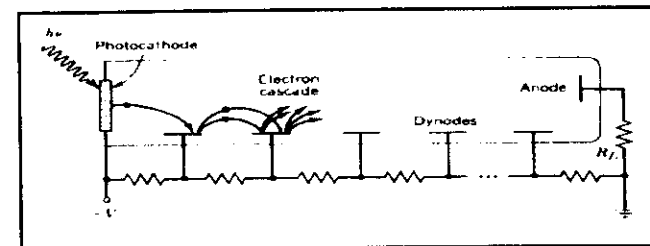


Fig. 6

When a primary electron with energy  $E_{pe}$  strikes the surface of a dynode,  $g$  secondary electrons are emitted;  $g$  is the dynode gain. If each dynode has same gain, the photomultiplier total gain is given by:

$$G=g^n \quad (17)$$

Fig. 7 shows the secondary emission ratio  $g$  for various dynode materials as a function of accelerating voltage for the primary electrons.

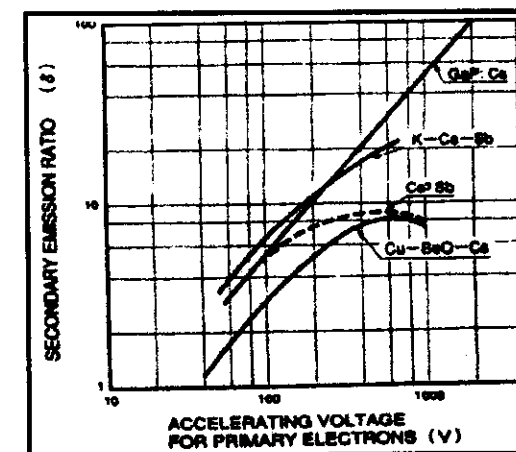


Fig. 7

All diagrams show a maximum which can be explained as follows:

- for low energies of the primary electron the energy transfer takes place at the surface of the dynode, the probability of emission is very high but the available energy only allows the ejection of a small number of secondary electrons.
- for high energies the primary electron is deeply absorbed and generates a high number of secondary electrons but they have little chance of escaping.

The maximum efficiency is obtained for intermediate energy values.

It is worth noting that the secondary emission process presents fluctuations and then noise, being the process statistical. Moreover the contribution to the total noise is negligible and compensated for internal high by amplification, as we will see.

### 5.1. Cathode- first dynode stage

This stage behaves largely as a vacuum phototube, the dynode being the equivalent of the anode. The most important function assigned to this stage is to collect with high efficiency the photoelectrons emitted from the photocathode; focusing electrodes are incorporated in order to guide the photoelectron from the photocathode to the first dynode by means of their electrostatic field.

Besides this stage may show a short response time; then all photoelectrons emitted from the photocathode at the same time should arrive simultaneously at the first dynode or at most with little time spread. For this purpose curved photocathodes are used in which the electron trajectories are of about equal length and acceleration (fig. 8).

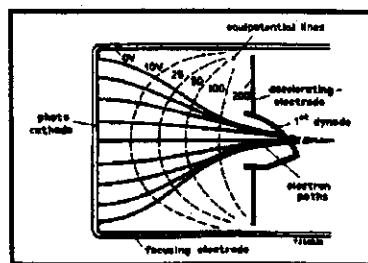


Fig. 8

### 5.2. Dynode chain

There are a variety of dynode types and chain structures and each type exhibits different features.

For the geometrical arrangement of the dynode chain, four main configurations are used; fig. 9 illustrates the relative cross sectional views.

It is essential to select the chain type in accordance with the desired application.

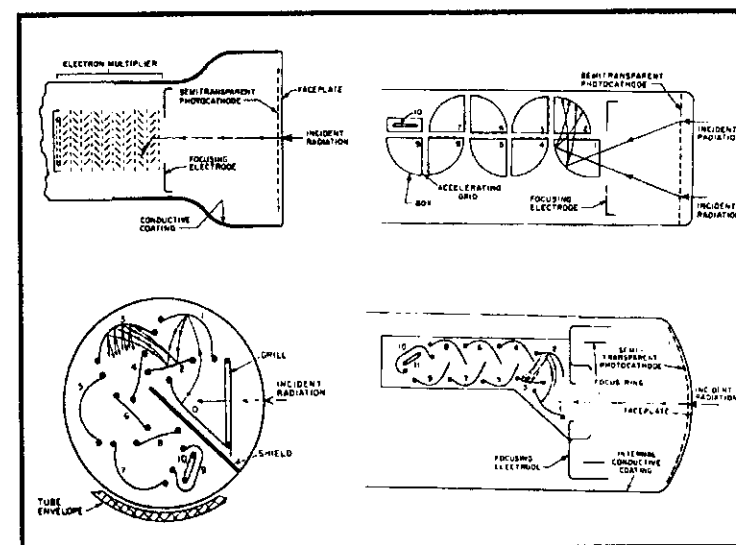


Fig. 9

### 5.3. Last dynode-anode stage

The anode is the electrode which collects the electrons from the last dynode. The anode often consists of a thin wire or grid mounted close to or inside the final dynode in order to minimize any capacitance effects. The electron current produced is the output signal.

Anode linearity is limited by two factors:

- the bleeder circuit which will be described later,
- the space charge effects due to a large current in the last stage; the result is a current saturation. The maximum anode current is quoted in the data sheets.

#### 5.4. Anode dark current

Anode dark current arises from the following causes:

- (i) thermoionic emission from the photocathode and dynodes,
- (ii) leakage current between the anode and the other electrodes inside the tube,
- (iii) fluorescence on the envelope material caused by scattered internal electrons,
- (iv) ionization of residual gases.

These currents should be kept as small as possible, the photomultiplier being a tube used for handling small amounts of light and current.

#### 6. Single Electron Response (SER)

The response of a photomultiplier to a light signal is made up of many pulses by single electrons. The SER of a photomultiplier may be obtained by recording the output pulse height distribution when the photocathode is illuminated by a weak light source. The electron leaving the photocathode strikes the first dynode where it is multiplied by means of secondary electron emission, this secondary emission is repeated at each of the successive dynodes and is finally collected by the anode.

The output current negative signal exhibits shape and amplitude which depend on the multiplication of the dynodes and the fluctuations of the transit time. The electronic charge is proportional to the current pulse area and represents the photomultiplier gain for the single electron considered. An important initial information is connected to the number of electrons collected by the anode for single electron emitted from the photocathode. This number is not constant, the multiplication process being statistical; its statistical distribution depends on the fluctuation in the cascade multiplication. Fig. 9 shows a histogram of the photomultiplier output pulse experimentally recorded by the multichannel analyser. The multichannel analyser (MCA) is an instrument that assigns the amplitude of input pulse to a channel. For example for a MCA with 1000 channels and 4 mV of

channel capacity it is possible to select pulses high from 4mV and 4 V. The abscissa indicates the pulse height. The mean value represents the mean gain of the tube that is the product of the mean secondary multiplication factor at each dynode. From the distribution of fig. 10 its variance, i.e. gain  $\sigma_G$  variance can be determined. This parameter is very important for understanding the intrinsic resolution capability of a photomultiplier; this is fundamental for measuring light levels or pulses with slightly differing amplitudes.

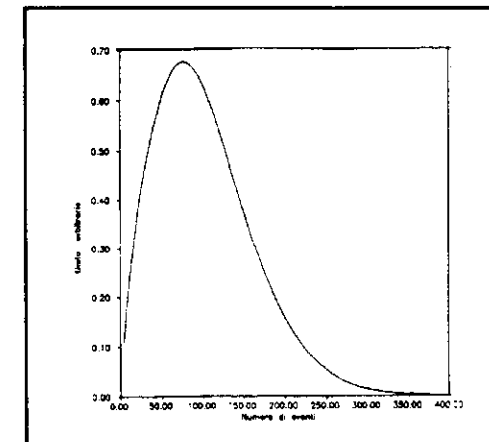


Fig. 10

Let us calculate this variance. The photons were assumed to be emitted according to a Poisson distribution. The conversion of photon into electrons and their collection by the first dynode and successively by other dynodes, are statistical processes of known distribution. The method of generatrix functions, being the process series in the cascade, can be applied to calculate easily the final result. We will leave reader to apply these functions as preferred, and will be the total variance found as follows:

$$\sigma_G = \sigma_1 + \frac{\sigma_2}{\alpha_1 g_1} + \frac{\sigma_3}{\alpha_1 g_1 \alpha_2 g_2} + \dots + \frac{\sigma_n}{\alpha_1 g_1 \dots \alpha_{n-1} g_{n-1}} \quad (18)$$

where  $g_i$  is the gain of the  $i_{th}$  dynode (mean value) and  $\alpha_i$  the collection efficiency from the  $i_{th}$  dynode to the  $i_{th}-1$ .  $\sigma_i$  is the variance of the  $i_{th}$  process of emission.

It is clear from equation (18) that the highest contribution to total variance is supplied by the first dynode, and their secondary multiplication factor has to be the

highest. For this reason the first dynode (photocathode-first dynode) is supplied with a voltage higher than the next. In this way values of  $g_1$  higher than  $g_2, \dots, g_{n-1}$  are carried out. This is obtained supplying the first stages with gradually decreasing voltages.

It is worth noting that Poisson statistics hypothesis is not always verified. The secondary emission process is in itself a Poisson distribution but with a mean value which varies for different points of the dynode. Therefore if the primary electrons hit the dynode over a large area, the secondary emission coefficient differs from place to place obeying a Polya distribution with higher variance. Therefore the best uniformity of the dynode surface and the best focalization between the dynodes are important.

### 7. Noise in the photomultiplier

The source of noise in the photomultiplier are as those present in the vacuum phototube. The amplitude distribution of noise pulses is shown in fig. 11.

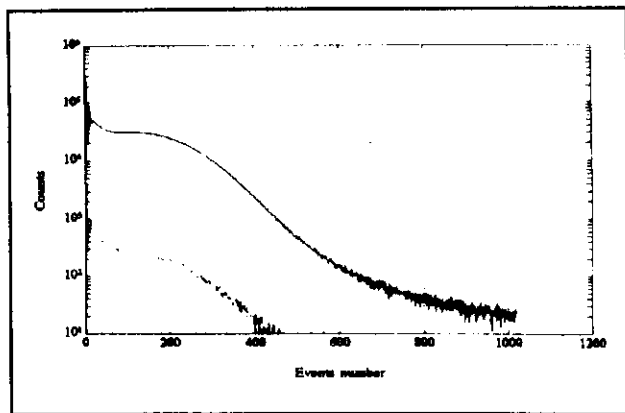


Fig. 11

It is different from the SER distribution mainly due to the presence of high number of small amplitude pulses and of a few very high pulses. The pulses in the first channels are those emitted from the dynodes, they are yielded from the electrons which do not have the full multiplication through the dynode chain. The higher pulses are produced by cosmic rays, ionic bombardment, etc.

### 8. Signal-to-noise ratio of photomultiplier tubes

In the case where Poisson multiplication statistics apply, if  $I_0$  is the mean current value from the photocathode to the first dynode, the mean square of shot noise at the output of multiplication chain, all stages being supposed equal to each other and with gain  $g$ , is given by:

$$\bar{I}_{\text{no}}^2 = 2eI_0g^n \sum_{i=0}^n g^i \Delta f \quad (19)$$

If  $I_s$  is the mean value of the current signal and  $I_d$  the mean value of the dark signal and  $4KT/R_L$  the noise associated to load resistance  $R_L$ , the current total noise is given by:

$$\bar{I}_{\text{no}}^2 = \left[ 2e(I_s + I_d)g^n \sum_{i=0}^n g^i + \frac{4KT}{R_L} \right] \Delta f \quad (20)$$

this expression is equal to that of a vacuum phototube except for the multiplying factor off the mean current. This factor is due to secondary multiplication.

The signal to noise ratio pertaining to the photomultiplier is expressed in root mean square as follows:

$$\begin{aligned} \frac{S}{N} &= \frac{e\eta g^n \Phi_s / \sqrt{2}}{\left[ 2e(I_s + I_d)g^n \sum_{i=0}^n g^i + \frac{4KT}{R_L} \right]^{1/2} \Delta f^{1/2}} = \\ &= \frac{e\eta g^n \Phi_s / \sqrt{2}}{\left[ 2e(I_s + I_d) \frac{g^n}{g^{2n}} \sum_{i=0}^n g^i + \frac{4KT}{g^{2n} R_L} \right]^{1/2} \Delta f^{1/2}} \\ \text{with } \Gamma &= \frac{1}{g^n} \sum_{i=0}^n g^i = \frac{g^{n+1} - 1}{g^n(g - 1)} \\ \text{for } g > 1 \text{ then } \Gamma &> 1 \end{aligned} \quad (21)$$

Suppose  $i=1$ . Comparing this relationship with that of equation for the vacuum photodiode it is clear that internal amplification reduces the weight relative to the thermal noise in the  $R_L$  of the gain square with respect to dark current. So, the photomultiplier signal to noise ratio is independent of the load resistance. Moreover it is a fast detector with very high sensitivity.

## 9. Time characteristics

When the photomultiplier tube is illuminated with a delta function radiation pulse of a stated amplitude, the output current pulse has a finite length and its barycentre is delayed as regards irradiating pulse. The amplitude, the shape and the delay of the output pulse fluctuate and also vary with the same input radiation pulse. The relation between the irradiating pulse and the mean output pulse represents the transfer function of the photomultiplier. This function also depends from on the spatial distribution of illumination at the photocathode. The resonse of the single electron emitted from the cathode is also useful for the time resolution of the photomultiplier. During the multiplication process, the travelling time of the electrons differs at the same stage, due to the difference of both the leaving points of the dynode surface and the starting speeds.

Rise time, pulse duration and transit time (fig. 12) are affected by the accelerating voltages between the dynodes.

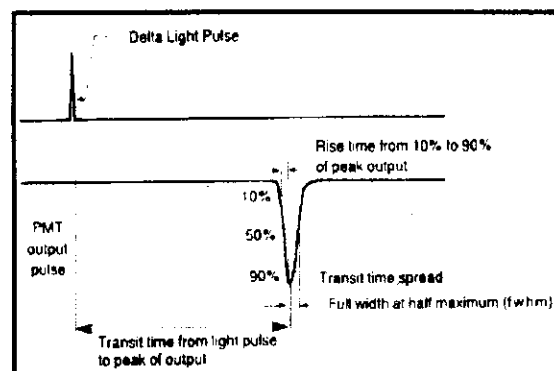


Fig. 12

In practice the output from the photomultiplier for a light pulse in input also depends on the geometry of the last dynode-anode stage, which must provide carry out the following:

- reduction of space charge.
- isochronism of electron trajectories.

- minimise action of electromagnetic induction produced in the anode by the electronic charge arrival.

Besides, for the detection of light pulses with fast rise and fall times a coaxial cable with  $50 \Omega$  impedance is used to make the connection between the photomultiplier tube and the output circuit.

## 10. Photomultiplier operation

A high voltage from 500 to 3kV is usually applied across the cathode and anode, with a proper voltage gradient between all the electrodes. The interstage voltage gradient is supplied by using voltage-dividing resistors connected between the anode and cathode, this circuit is known as a voltage divider circuit or bleeder circuit, see fig. 13.

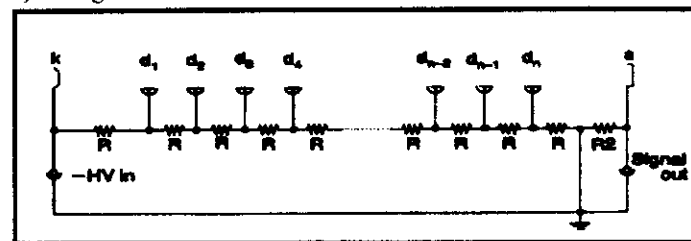


Fig. 13

Current  $I_b$  is approximately the applied voltage  $V$  divided by the sum of the resistor value as follows:

$$I_b = \frac{V}{R_1 + R_2 + \dots + R_n} \quad (22)$$

The Zeener diodes can be used to maintain the interstage voltages at constant values for stabilizing the interstage voltages mainly between photocathode and the first dynode.

Generally the anode is grounded and a large negative voltage is applied to the photocathode. This configuration avoids the potential voltage difference between the external circuit and the anode. Besides the anode is the electrode where the output signal is taken, so that, for safety reasons, this configuration is better. With the grounded cathode configuration, a coupling capacitor  $C_c$  must be used to separate the positive high voltage applied to the anode from the signal and so

eliminating the continuous component. Moreover this configuration makes it impossible to extract a DC signal (fig. 14).

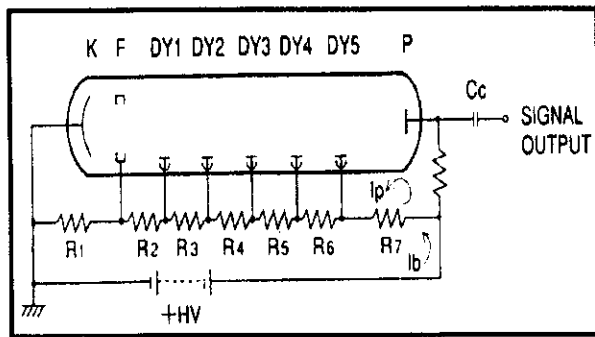


Fig. 14

In every configuration, if the light level over the photocathode increases, the relationship between the incident light and the anode current deviates from linearity and the tube saturates (fig. 15).

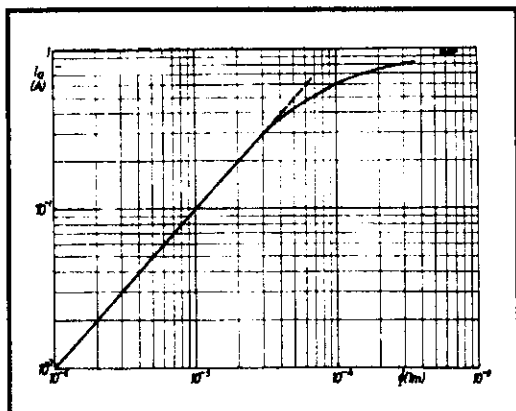


Fig. 15

The anode current and dynode current flow act to reduce the bleeder current. This reduction can be ignored if the anode current is small.

The gain of the photomultiplier is given by:

$$G = g^n \quad (23)$$

The secondary emission factor is linear with interstage voltage, dynodes working in the first length of secondary emission characteristics.

$$g = KV; \quad G = K^n V^n = KV^n \quad (24)$$

A variation  $\Delta V$  of the voltage produces a variation of the gain given by:

$$\frac{\Delta G}{G} = n \frac{\Delta V}{V} \quad (25)$$

so small variations of the supply voltage produce variations of the gain  $n$  times higher. So a stabilized power supply is required.

Now let us discuss the bleeder. In applications where a high linear output is required, the voltages between the electrodes do not feel the signal presence effects. This means that all the currents which are collected on the dynodes and so enter the bleeder circuit, can be smaller than the bleeder circuit quiescent current  $I_Q$ , so called because it refers to the current that flows in the bleeder circuit under operating conditions but in the absence of an external applied signal.

Very high current ending up in the dynodes causes voltage variations in the bleeder circuit, which depend on the signal level. This causes non linear output. It is opportune to examine two situations:

a) DC operation

In this case :

$$\frac{\Delta G}{G} \approx \frac{I_s}{I_r} \quad (26)$$

This means that in order to have gain variations less than 1%, the signal current cannot be better than 1% of the bleeder circuit quiescent current or, likewise is the same, the bleeder current must be almost 100 times greater than that throught out from the optical signal. This condition greatly restricts the highest current value which can be utilized, the bleeder current being limited by both, the highest current value from the power supply and the maximum dissipation provided by the bleeder circuit.

It is pratically impossible to utilize quiescent currents greater than a tenth of mA.

b) Pulse operation

When a photomultiplier tube is pulse operated, the circuit of fig. 13 cannot be used above a fraction of a bleeder current for maximum linear output. The coupling capacitor can be connected to the last few stages in order to overcome this problem

fig. 16.

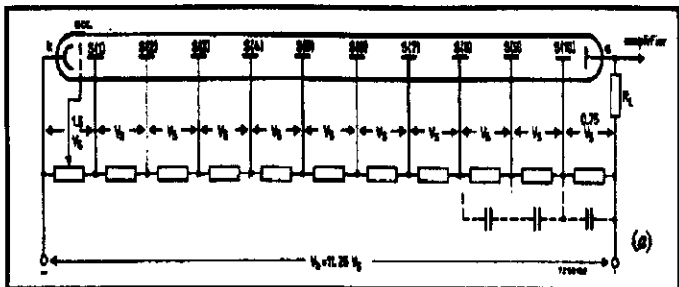


Fig. 16

These capacitors supply the photomultiplier with an electric charge during pulse duration and restrain the voltage drop in the last stage, so improving pulse linearity.

Let us calculate the capacitors value at the last stage. With the anode pulse peak voltage  $V_a$  and pulse width  $t_w$ , the load resistance  $R_L$ , the interstage resistor values  $R_{n-2}=R_{n-1}=R_{L,n}$  and the bleeder current  $I_b$ , anode charge  $Q_a$  per pulse is given by:

$$\begin{aligned} Q_a &= t_w \frac{V_a}{R_L} \\ Q_3 &= t_w \frac{V_3}{R_3} \\ Q_2 &= t_w \frac{V_2}{R_2} \\ Q_1 &= t_w \frac{V_1}{R_1} \\ C &= \frac{Q}{V} \end{aligned} \quad (27)$$

Let us calculate the capacitor values being linearity of 1%

$$\begin{aligned} Q_3 &\geq 100 \cdot Q_o \\ C_3 &\geq \frac{Q_3}{V_3} \geq 100 \cdot \frac{Q_o}{V_3} \\ C_2 &\geq \frac{Q_2}{V_2} \geq 100 \cdot \frac{Q_o}{V_2} \\ C_1 &\geq \frac{Q_1}{V_1} \geq 100 \cdot \frac{Q_o}{V_1} \end{aligned} \quad (28)$$

Assuming  $g$  between the dynodes will result:

$$Q_2 = \frac{Q_3}{g} ; \quad Q_1 = \frac{Q_3}{g^2} \quad (29)$$

Then the capacitance values of  $C_2$  and  $C_1$  result:

$$\begin{aligned} C_3 &\geq 100 \cdot \frac{Q_o}{V_3} \\ C_2 &\geq \frac{100}{g} \cdot \frac{Q_o}{V_2} \\ C_1 &\geq \frac{100}{g^2} \cdot \frac{Q_o}{V_1} \end{aligned} \quad (30)$$

Where:

$$V_1 = I_b R_{n-2} ; \quad V_2 = I_b R_{n-1} ; \quad V_3 = I_b R_n ; \quad (31)$$

Then:

$$\begin{aligned} C_3 &\geq 100 \cdot \frac{Q_o}{I_b R_n} \\ C_2 &\geq \frac{100}{g} \cdot \frac{Q_o}{I_b R_{n-1}} \\ C_1 &\geq \frac{100}{g^2} \cdot \frac{Q_o}{I_b R_{n-2}} \end{aligned} \quad (32)$$

Practically capacitance values of 10 times larger than the calculate value can be applied.

Often output saturation will occur when the incident light is increased while the voltages are fixed. In order to avoid space charge effects the voltage applied to the each stages where space charge effect is present, the output linearity will be guaranteed measuring the resistor value. This circuit was called "tapened bleeder".

## 11. Image-Intensifier technique

An image intensifier is necessary to keep the bundle of electrons in spatial forms so that the position in which the bundle strikes the phosphor has a one-to-one relationship with the point of origin.

An image intensifier provides the following function:

- 1) It converts photons to electrons.
- 2) It increases the energy of these electrons while keeping them in spatial focus.
- 3) It multiplies the number of electrons (i.e. microchannel plate).
- 4) It converts the energy of the resulting electrons into a visual image.

The photocathode is used to convert photons to electrons.

Focusing is achieved either by electrostatic elements or by a magnetic field parallel to the axis of the tube.

The resolution obtained using magnetic field focusing is superior to that obtained with electrostatic focusing. Resolution of from 10 lp/mm to 30 lp/mm are common.

## 12. Gain

Let's calculate the gain of a single-stage image intensifier, the gain being the ratio of the number of photons emitted at the output  $N_o$  to the number of photons incident on the cathode  $N_i$ . The number of electrons emitted from the cathode depends on quantum efficiency  $\eta$ . These electrons will be accelerated by voltage  $V$  between the photocathode and the phosphor. The electron will be converted to photons of energy  $h\nu$  according to phosphor efficiency  $\epsilon_p$ . The number of photons emitted will be given by:

$$N_o = N_i \frac{\epsilon_p V \eta}{h\nu} \quad (33)$$

The gain is:

$$G = \frac{N_o}{N_i} \quad (34)$$

For example with:  $\eta=0.15$ ,  $V=10^4$  Volt,  $\epsilon_p=0.10$  and  $h\nu=2.8$  Volt;  $G=50$

Various methods are available to achieve the electron multiplication required in this type of device. Many different devices have been developed to enable one to see in conditions of extremely low level intensity, such as that from the stars.

## 13. Zero generation of image intensifier tube

Fig. 17 shows an image intensifier of zero generation.

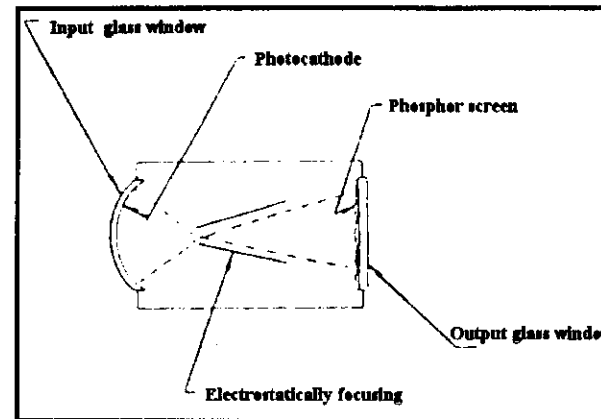


Fig. 17

Light from the object is focused onto the input to the tube by means an optics system and transmitted through the window onto the semitransparent photocathode. A corresponding electron pattern is emitted. A voltage of up to 16 kV accelerates these electrons on a phosphor screen where the electron pattern becomes a photon pattern, which is transmitted through the output window.

The typical luminance gain is about 35.

## 14. First generation of image intensifier tube

With the development of optical fibres, single stage electrostatically-focused intensifier were coupled in cascade (fig. 18).

The three stages of the cascade intensifier together require 40 kV. This derives from an oscillator, encapsulated with the intensifier, operating from a low-voltage d.c. supply.

Typical gains are between  $3 \cdot 10^4$  and  $5 \cdot 10^4$ .

The P20 type phosphor is usually used. Its persistence is a few milliseconds for a single stage tube. In a three stages tube the afterglow remains visible for several seconds as a result of amplification. Image persistence is a limitation of first generation image intensifiers.

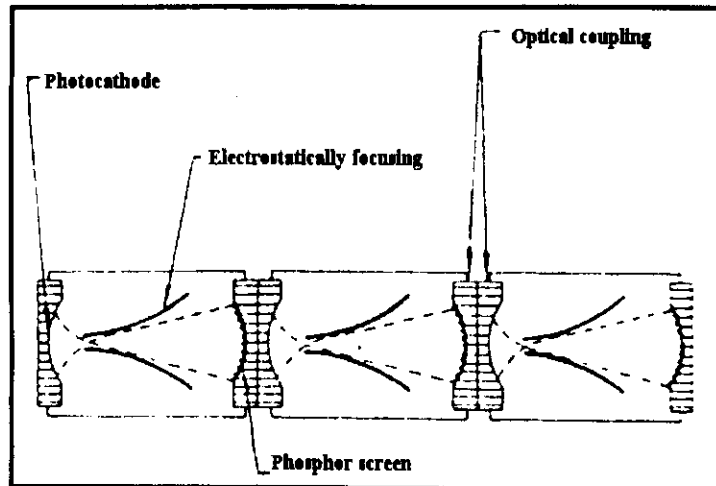


Fig. 18

### 15. Second generation of image intensifier tube

This type is derived from zero generation. Channel lumen gains of up to  $10^3$  can be reached in a single tube by placing a channel plate between the photocathode and phosphor screen.

Such a single tube has the following advantages over a conventional cascade system:

- The overall length of the system is shorter.
- The operating voltage is only 10 kV compared with 45 kV for a cascade of three tubes.
- The resolution is better because the tube consists of only two elements, the channel plate and the screen compared with six fibre optic windows and three screens of a three-stage tube.
- The gain can be adjusted without altering the image quality.

There are two main types of channel image intensifiers: the **proximity tube** (fig. 19) and the **inverter tube** (fig. 20).

They differ in the method of coupling the photocathode and channel plate.

In the proximity focused tube (fig. 19) the photocathode is placed as close as possible to the plate and high electric field restricts the lateral spread of the electrons. This gives the shortest possible tube and distortionless reproduction. However, there is an appreciable loss in resolution due to the lateral spread of electrons and expensive manufacturing techniques are required for producing a photocathode so close to the plate.

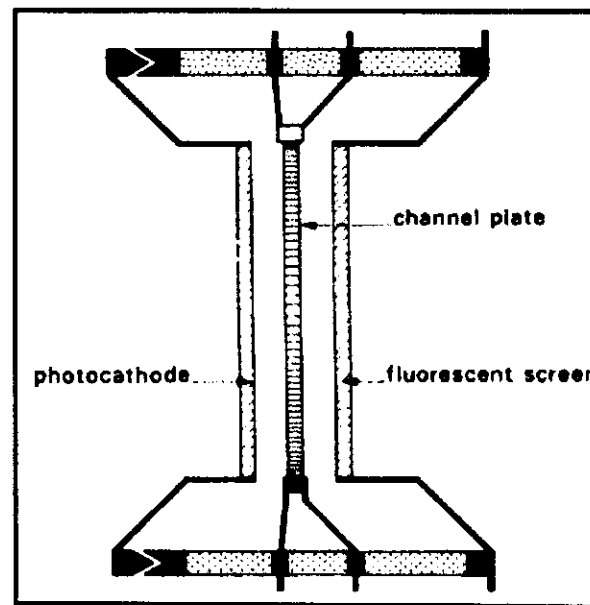


Fig. 19

In the inverter tube (fig. 20) an inverting electron lens transfers the image from photocathode to the plate without any significant loss in resolution but with some pincushion distortion. The inverter tube is longer, but for most applications some form of image inversion is necessary to compensate for the inversion of the

objective lens. The length of a proximity tube with an inverting system, such as "twister" fibre optics, is only slightly less than that of an inverter tube.

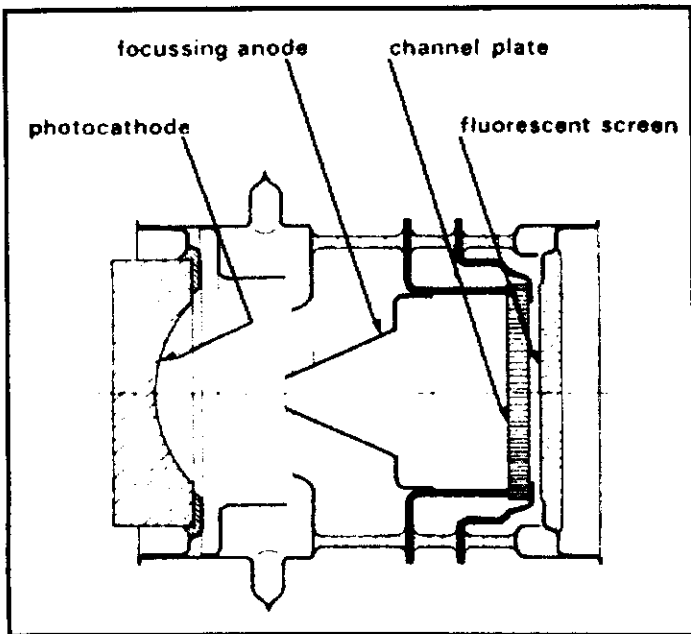


Fig. 20

Besides the design and performance itself the inverter tube will be described.

### 15.1 Electrons lens of image intensifier inverter tube

A channel image intensifier imposes one major design restraint on the electron lens; the image plane must be flat to match the channel plate. This means that a curved fibre optic photocathode window must be used. In the VX 8565 the lens has been restricted to a simple diode construction, i.e. each electrode is at the same potential as either the photocathode or the plate. This design thus reduces to a compromise between overall length and image distortion. This compromise cannot be made without considering the associated optics because the pincushion distortion in the electron lens is compensated, to a large extent, by the barrel distortion inherent in the objective optical lens.

### 15.2 Channel plate of image intensifier inverter tube

A microchannel-plate electron multiplier consists of an array of tubes, or channels, fused in the form of a thin disc (fig. 21). When used as an intensifier, an electron image projected on one face of the plate appears at the second face amplified by a factor of at least  $10^3$ . The operation of the channel plate is best described in terms of that of a single-channel multiplier; that is, in terms of one unit of the matrix.

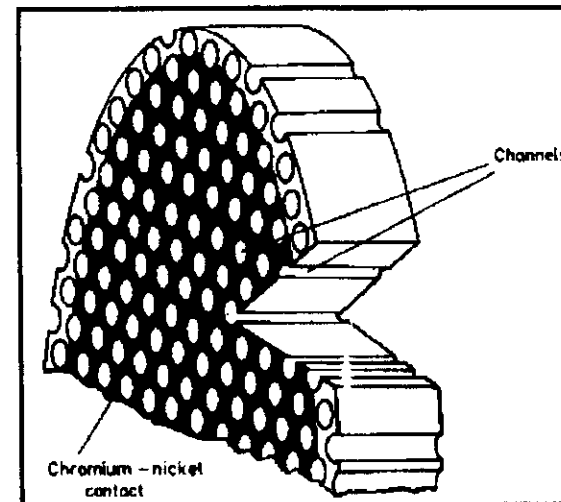


Fig. 21

Single-channel electron multipliers have been successfully used for a number of years for the detection of electrons, ions, ultraviolet radiation, and X-rays. They offer several advantages over conventional discrete-dynode multipliers; in particular, high electron gain, low background count rate, and low power consumption, coupled with ruggedness, small physical size, and simplicity of use. The principle of operation of the single-channel multiplier is illustrated in Fig. 22.

The channel consists of a hallow glass tube, about 1 mm diameter, with an internal resistive surface processed to have a high secondary emission coefficient. The multiplier is operated in a vacuum with a potential difference applied between electrodes at the ends of the tube. When an electron, or some other charged particle or quantum, enters the low-potential end of the tube and collides with the wall, several secondary electrons are produced. These are accelerated by the applied

axial field and in turn produce more secondaries. This process is repeated many times along the channel, and a large number of electrons ( $\approx 10^8$ ) finally leave the high-potential output.

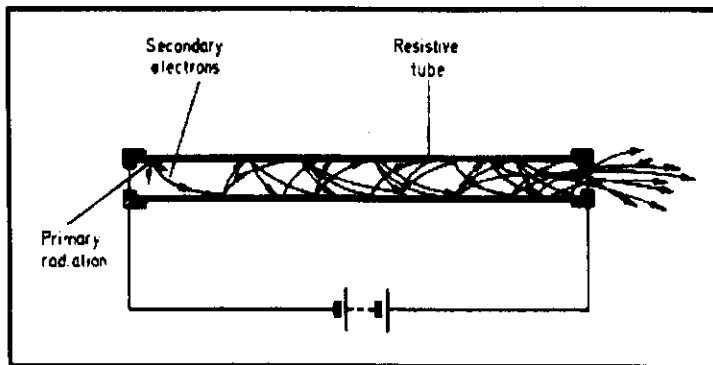


Fig. 22

The electron gain of the channel depends on the applied voltage, on the ratio of channel length to diameter, and on the secondary emission characteristics of the channel surface. Typically, gain increases from about  $10^3$  at 0.9kV to more than  $10^8$  at 3kV. Because gain is determined by the length-to-diameter ratio of the channel and not by its overall size, the dimensions can be scaled down without affecting performance. Thus, very small multipliers whose dimensions are limited only by the technology and the ability of the channel material to withstand electrical breakdown can be made.

By constructing a parallel array of straight single-channel multipliers, each having an internal diameter of about 25  $\mu\text{m}$ , a device can be made which will amplify an electron image. Such a device is called a channel-plate electron multiplier, or microchannel plate (MCP). It is normally operated at about 1 kV and has a gain of at least  $10^3$ , typically  $3 \times 10^3$ .

An important parameter of the channel plate is the size of the channels. The effect of channel size on the resolution will be discussed in greater detail later, but as a first approximation the smaller the channels the better the resolution.

As a channel size is reduced the thickness of the plate decreases if the length-to-diameter ratio of about 40 is to be maintained. As the applied voltage for a given gain remains the same the electric field strength in the channel is increased. It is

gain remains the same the electric field strength in the channel is increased. It is this factor which finally limits the channel size. Channel plates with a pitch of 12  $\mu\text{m}$  can be made by current manufacturing processes and these have been operated in image intensifiers. Such tubes have a resolution which is significantly greater than any other high gain intensifier.

The axes of the channels are generally tilted a few degrees to the perpendicular to the channel plate face. This prevents ions generated in the channel plate-screen region, where the current densities are highest, getting back to either the input of the channel plate or the photocathode. In both cases spurious electron pulses would be generated and ions striking the cathode reduce its sensitivity.

### 15.3 Phosphor screen of image intensifier inverter tube

The choice of phosphor screens in a cascade of three identical tubes is restricted because the energy conversion between phosphor and photocathode must be as efficient as possible. The choice of the phosphor screen of a channel tube is less restricted. Provided it has good resolution the gain of the channel plate can be increased to compensate for reduced efficiency. In this way a phosphor of any colour or decay characteristics can be used.

### 15.4 Modulation transfer function of image intensifier inverter tube

The usual method of describing the resolving properties of image devices is by the modulation transfer function (MTF). If a resolution pattern with 100% contrast and a particular spatial frequency is projected onto the input of an imaging system it will be reproduced at the output with less contrast. The MTF is a graph of the output contrast against spatial frequency.

This approach must be used carefully with channel plates because as the input spatial frequency approaches the repetition or array frequency of the channels, moiré fringes will be formed and the output pattern will have a different orientation and spatial frequency to the input.

## 16. Third generation of image intensifier tube

The major difference between second and third generation is the photocathode, second generation use a multialkali photocathode.

In third generation a GaAs and AlGaAs photocathode is used.

## Laboratory Guide

### Introduction:

The laboratory work concerns three experiments which involves the utilization of a photomultiplier and an image intensifier tube.

The photodetectors features to be determined are the following:

- 1) The type of photocatode. That is its spectral response for a broad band source.
- 2) The signal to noise ratio (S/N) or the noise equivalent power (NEP). That is the minimal signal to obtain an S/N equal to one.
- 3) The single electron response (SER) observation with the oscilloscope and a Multichannel analyser (MCA).
- 4) The noise figure of an image intensifier tube. That is a figure of merit which characterizes the loss of information of the final pattern.

### Instruments background:

In these experiments the use of both electronic instrumentation and a computer software provides for the signal acquisition and the monochromator movement. Below the main features of these instruments and their use will be described.

#### 1) *Acquisition driver:*

Actually, a multifunction board provides for interface a lot of instruments to computer. A data acquisition module allows to the computer to accept both analog and digital signals, and to produce output signals outside the range of buffered TTL levels, or in forms such as current or frequency.

In the described experiments, a multifunction board is used for both:

- a) acquire the analog signals from the photodiode and from the photomultiplier
- b) control the movements of the monochromator.

The PCI-20098C Multifunction Carrier of Burr Brown provides the following features:

- 16 single-ended or differential<sup>1</sup> analog input channels.
- 16 digital I/O channels with or without handshaking<sup>2</sup>.
- 2 16-bit counters which can be concatenated to operate as one 32-bit counter.
- A DMA controller for transferring analog input data to the PC under DMA control.
- A PC interrupt<sup>3</sup> controller for generating various level interrupts to the PC from a variety of source.
- A wait state generator that extends the PC bus cycle for interfacing with slower devices.

To utilize the carrier performance a software drivers like that using the GWBasic language code, are used.

## 2) Monochromator:

It is an optical instrument which allows to isolate a narrow part of the spectrum of a source; the basic of the monochromator used is a groove density diffraction grating. The groove spacing is a parameter which determines the longest wavelength could possibly get in first order. The diffraction equation is:

$$a[\sin(i) + \sin(d)] = m\lambda \quad (1)$$

where:  $a$  = the groove spacing

$i$  = the angle of incidence

$d$  = the angle of diffraction

$m$  = the order of diffraction

$\lambda$  = the wavelength

We consider the first order,  $m=1$ . For example, which a 1200  $1/\text{mm}$  grating,  $a=833\text{nm}$  the maximum possible value of  $\lambda$  to satisfy eq.(1) is obviously 1666 nm, with the maximum possible value of  $\sin(i) + \sin(d)$  is 2 being  $d \approx 90^\circ$  and  $i \approx 90^\circ$ .

<sup>1</sup>Single-ended means which all channels are referred at the same ground; differential means which the data are the difference between two signal channels, that is the value is not related to each ground.

<sup>2</sup>Handshaking means which is possible to use the signal I/O between Board and instrument to check, for example the start, stop, end of the data envoi.

<sup>3</sup>The PC interrupt is utilized for command the various levels command to CPU so that it execute a subroutine.

This theoretical performance is reduced by some factors. In the commercial monochromator the angle was limited to  $45^\circ$ , this is a mechanical limit. A grating produces a lot of diffraction orders, therefore in order to enhance the first order efficiency the grating was blazed; this grooves shaping techniques allows to optimize the grating at one specific wavelength but reduces the efficiency to theoretical range. For this reason it is very important to specify the usable and primary efficiency ranges list of a single grating. The usable range is that in the first order for which the efficiency grating is more than 10% (for unpolarized radiation) and the primary is the range in which the grating has an efficiency of more than 20% (for unpolarized radiation). So there are three spectral ranges:

- 0 nm to the theoretical maximum.
- Maximum range determined by the mechanical rotation limit of the monochromator.
- The efficiency limited spectral range somewhat arbitrarily divided into primary ( $>20\%$ ) and usable ( $>10\%$ ).

A typical grating efficiency curve is shown fig. 1:

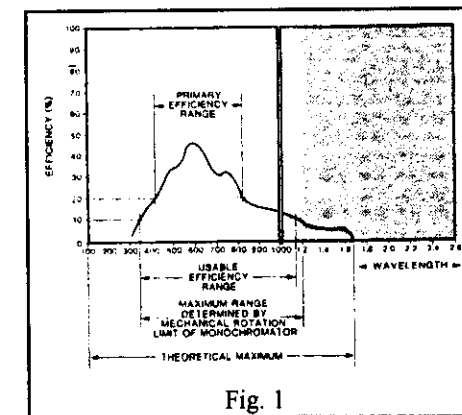


Fig. 1

The diffraction efficiency usually depends on the polarization of the radiation incident on the grating. For the monochromators used, the linearly polarized

radiation with the electric vector parallel to the grooves is **p** polarized and radiation polarized perpendicular to the grooves is **s** polarized. Therefore most of graphs for any grating have three separate efficiency curves, one for incident unpolarized radiation, the second for radiation polarized parallel to the grooves, and the third for radiation polarized perpendicular to the grooves. Typically the efficiency curves for **p** polarized light peak is slightly lower than nominal blaze wavelength and smoothly declines to 0 at about three times the blaze. The curves for **p** polarized light are generally smooth, without dramatic changes in direction or sharp features. The curves for **s** polarized light peak are slightly above nominal blaze and decline but can recover dramatically and show good efficiency right out to the theoretical maximum diffraction wavelength; **s** is the polarization curve, particularly for blaze angles in the 8-15° range, can sharp features, **anomalies**. The curve efficiency of used grating is shown in the fig. 2.

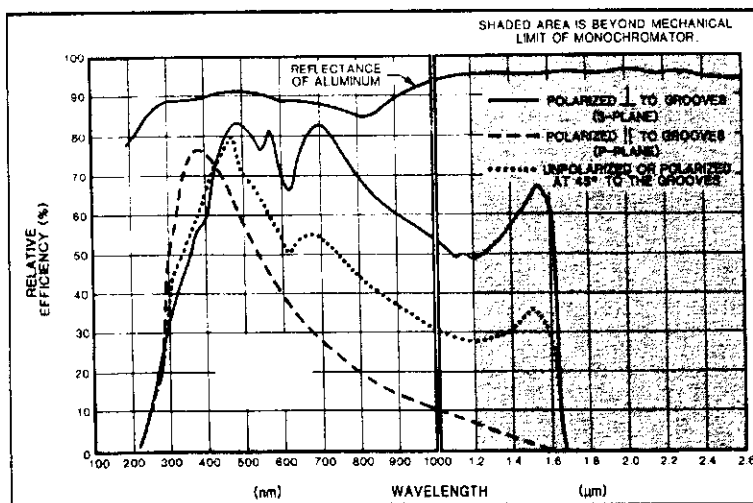


Fig. 2

This grating has the following features: groove density = 1200 l/mm, blaze wavelength = 500 nm, reciprocal dispersion = 2.86 nm/mm, primary and usable wavelength range = 300-1200 nm.

The optical system for the actual monochromator is an in-plane unsymmetrical Czerny-Turner configuration. This is illustrated in the fig.3. When the exit slits are placed unsymmetrically with respect to the grating, the zero coma point is located within the working wavelength range, so a significantly reducing coma throughout the range. Mirrors M3 and M4 may be rotated into or out of the input and output optical paths to allow the use of either the parallel or the in-line ports shown in the fig. 3.

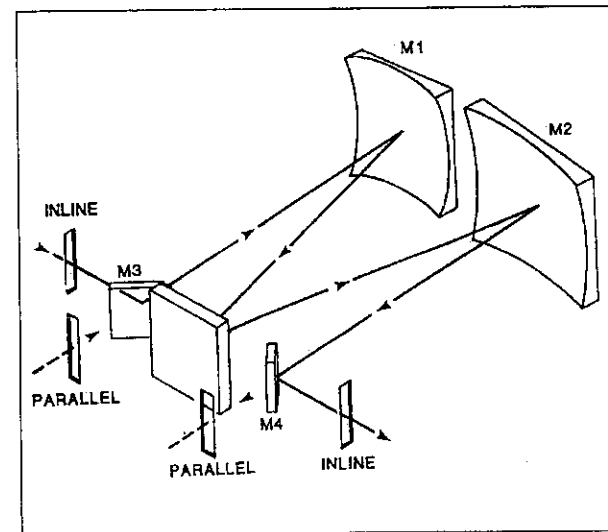


Fig. 3

### 3) Semiconductors photodiode:

The semiconductor photodiodes are based on the internal photoelectric effect; that is, the absorbed radiation creates electron-hole pairs, that remain inside the material producing at the output a current proportional to the incident radiation.

These detectors consist either of a uniform material or of a junction between two dissimilar materials. The latter involves *photovoltaic* mode, that is the may be used unbiased, or *photoconductive* mode, that is the junction externally reverse-biased.

In this experiment, only junction photodiode in photovoltaic mode will be used, where the dark current is considerably smaller than in the biased mode. This is

important for low level measurement. Besides photodiodes with large area (of about 1 cm<sup>2</sup>) exhibit linearity of responses mainly in photovoltaic mode.

The output current for photodiode is  $I = I_d + I_p$ , where  $I_d$  is the dark current and  $I_p$  the photocurrent proportional to the incident radiation flux. The photovoltaic working mode can be analysed by the circuit of fig. 4 for a constant irradiance where  $R_L$  is a load resistance and  $I_p$  is represented with an ideal current generator. Considering the circuit of fig. 4 we have:

$$V = -IR_L + V_0 \ln\left[1 + \left(I_p - I\right)/I_s\right] \quad (2)$$

where:  $V_0 = KT/c$ ;  $I_s$  = Reverse saturation current.

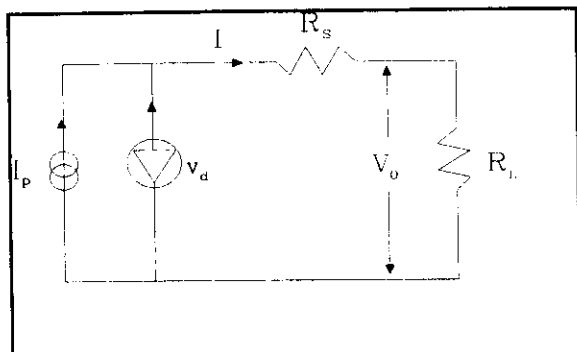


Fig. 4

The external voltage can be a logarithmic function of the incident light, or linear function  $V = V_d$  it depending of the value of  $R_L$ .

#### 4) Photomultiplier:

We will be use a Philips 56TVP photomultiplier tube. This is a 14 stage photomultiplier tube, which it have the follow features:

- Maximum voltage supply is 2750 Volt.
- Anode dark current is 5.0  $\mu$ A at the max gain ( $G=10^8$ ).
- Supply voltage for  $G=10^8$ , at 25°C temperature is 2500 Volt.
- Radiant sensitivity is 65 mA/W and 12 mA/W at 400nm and 700nm respectively.

- Linearity between anode pulse amplitude and input light pulse up to 100 mA.

For the generally information on the basic principles of a photomultiplier see the issue of the lectures.

#### 5) Image intensifier tube:

We will be use a Thompson TH934V1 image intensifier tube. This is a 2nd generation tube, which has the follow features:

- Temperature operating between -55° to +55° C.
- Dc input voltage between 2.0 to 3.0 Volt.
- Maximum luminance gain 50.000 fL/fc.
- Typical equivalent background illumination  $10^{-7}$  lux.
- Resolution at the center is 28/32 lp/mm and MTF is 4%.

For the generally information on the basic principles of a photomultiplier see the issue of the lectures.

#### Experiments description:

##### A) Spectral Sensitivity of photomultiplier

The experimental setup is shown in the fig. 5.

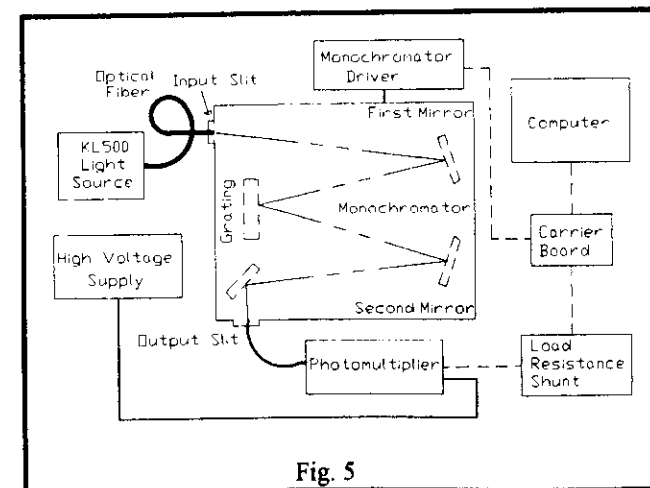


Fig. 5

The light source is the KL500 illuminator, it is coupled at the input slit of monochromator by an optical incoherent fibers.

The power light is attenuated by means of the neutral filters.

The photomultiplier tube is coupled to the output slit of monochromator by means of a single optical fiber.

The monochromator select wavelengths from 300 to 900 nm by step of 1 nm.

It is important to select, before, the best value of load resistance in order to have an output voltage signal less than 10 V; which is the highest value of working for the analog\digital converter.

The spectral distribution of source ( $P_S$ ) and the grating efficiency ( $\xi_G$ ) well-known; the measurements regard the incident flux on the output of the monochromator.

Then plot of the photomultiplier output current ( $I_{PH}$ ) vs. the luminance flux, will be obtain the spectral response curve of this photocathode. The  $I_{PH}$  is given by the output voltage  $V_{OUT}$  to load resistance  $R_L$  ratio.

#### **B) Noise Equivalent Power (NEP)**

Using the same previous experimental setup, it is need to select with monochromator the highest wavelength for value detected by photomultiplier.

The measurement starts without any light signal. Successively the power light is switching and will be attenuate in order to improve the same output signal than in dark condition.

The power light keep the value of percentage of filter attenuation.

It is possible to repeat the same measurement with the same photomultiplier cooled by means the Peltier effect.

The difference of dark signal is evident.

#### **C) Single Electron Response (SER) observing**

For this experience it will use the same cooled photomultiplier; the experimental arrangement is shown in the fig. 6.

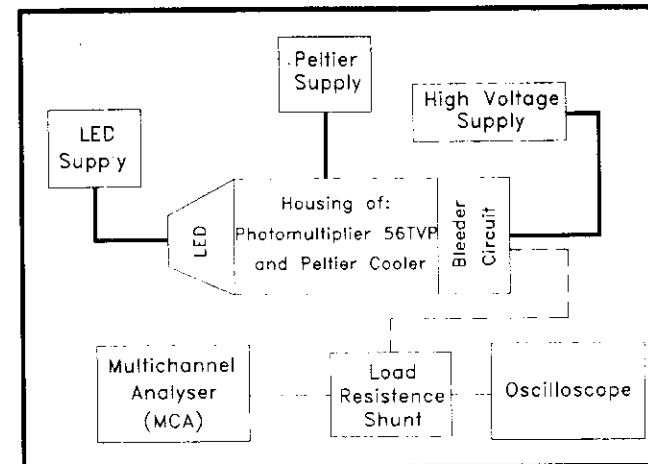


Fig. 6

In order to determine the total number of pulses whose heights fall in channels throughout the range of the pulse heights a MultiChannel Analyser (MCA) can be used at the output of the photomultiplier tube.

The MCA consists of some of the following elements:

- a section that associates each pulse with a specific amplitude channel,
- a memory for the number of pulses in each channel,
- a display that gives information about data stored in the memory.

The system employs pulse height-to-time converter.

#### **D) Use of an second generation image intensifier**

Appendix: A. Single current on the different dynodes of photomultiplier tubes

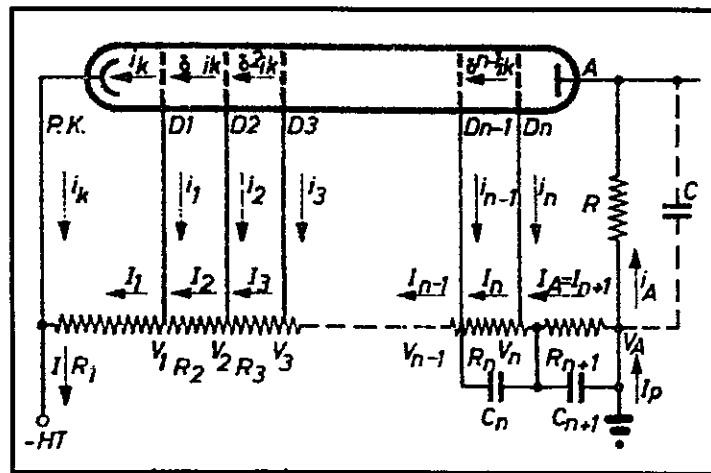


Fig. 7

Referring fig. 7, it is:

$$i_1 = g_1 i_k - i_k = (g_1 - 1) i_k \quad (3)$$

The first Kirckhoff's law applied to a dynode is: the sum of the current arriving at any point in a network is equal to the sum of the current flowing away from it:

$$\begin{aligned} i_2 &= g_1 g_2 i_k - g_1 i_k = (g_2 - 1) g_1 i_k \\ i_3 &= (g_3 - 1) g_1 g_2 i_k \\ &\vdots \\ i_n &= (g_n - 1) g_1 \dots g_{n-1} i_k \\ i_A &= g_1 \dots g_n i_k = G i_k \end{aligned} \quad (4)$$